Available online at www.sciencedirect.com
ScienceDirect
Bioorganic & Medicinal Chemistry Letters
Bioorganic & Medicinal Chemistry Letters 16 (2006) 5127–5131

Synthesis and biological evaluation of benzamides and benzamidines as selective inhibitors of VEGFR tyrosine kinases

Hiroyuki Nakamura,[a,*] Yusuke Sasaki,[a] Masaharu Uno,[a] Tomohiro Yoshikawa,[a] Toru Asano,[a] Hyun Seung Ban,[a] Hidesuke Fukazawa,[b] Masabumi Shibuya[c] and Yoshimasa Uehara[b]

[a]*Department of Chemistry, Faculty of Science, Gakushuin University, Tokyo 171-8588, Japan*
[b]*Department of Bioactive Molecules, National Institute of Infectious Diseases, Tokyo 162-8640, Japan*
[c]*Institute of Medical Science, University of Tokyo, Tokyo 108-8639, Japan*

Received 23 March 2006; revised 26 June 2006; accepted 11 July 2006
Available online 8 August 2006

Abstract—A series of benzamidines and benzamides was synthesized as selective inhibitors of vascular endothelial growth factor receptor (VEGFR) tyrosine kinases, and tested for inhibitory activity toward autophosphorylation by the enzyme assay. Selective inhibition of VEGFR-2 tyrosine kinase was observed in the salicylic amide **4e** and the anthranilic amidine **5a**, and their percent inhibitions of VEGFR-2 tyrosine kinase were 44–60% at a 10 μM concentration of compounds. The salicylic amide **4a** showed inhibition of both VEGFR-1 and VEGFR-2 tyrosine kinases at a 10 μM concentration.

Angiogenesis is tightly regulated and only occurs normally in inflammation, wound healing, and the female reproductive cycle in the adult.[1] Uncontrolled angiogenesis involves pathological states such as atherosclerosis, diabetic retinopathy, rheumatoid arthritis, and solid tumor growth. Vascular endothelial growth factor (VEGF) is a key growth factor in tumor angiogenesis, therefore, its receptor tyrosine kinases known as VEGFR-1 (Flt-1) and VEGFR-2 (KDR/Flk-1) have been considered as attractive targets for development of anti-cancer drugs.[2] Various small molecule VEGFR kinase inhibitors have been developed, such as SU6668,[3] ZD6474,[4] PTK787,[5] AAL993,[6] the pyrazine-pyridine compound **1**,[7] and aminopyrimidine **2**[8] (Fig. 1). We focused on the anthranilic amide framework of AAL993. According to the X-ray structural analysis, AAL993 interacted with VEGFR2 kinase domain through hydrogen bonds between the pyridine-N and the backbone-NH of Cys919 in the hinge region of the kinase, the anthranilamide–C=O and the backbone-NH of Asp1046 of the DFG-loop, and the anthranilamide-NH with the side-chain carboxylate of Glu885 of helix-C as well as the pseudocycle formation by an intramolecular hydrogen bond between the aniline–NH and the benzanilide–C=O.[9] We are interested in *an amidine skeleton* as a mimic of an amide. Amidines are, in general, more basic in comparison with ammonia, therefore expected different properties from the corresponding amides. Previously, we synthesized 4,5-dimethoxyanthranilic amides and 4,5-dimethoxyanthranilic amidines as a mimic of the 4-anilinoquinazoline framework for inhibition of epidermal growth factor receptor (EGFR) tyrosine kinase.[10] In this paper, we synthesized a series of the benzamides (**3** and **4**) and benzamidines (**5** and **6**) (Fig. 2), and evaluated their inhibitory activity of VEGFR1/2 tyrosine kinases.

Anthranilic amides **3a–f** were synthesized from methyl 2-aminobenzoate **7a** and methyl 4,5-dimethoxy-2-aminobenzoate **7b** as shown in Scheme 1. Reductive amination reactions of **7a** and **7b** with 4-pyridinecarboxaldehyde gave the corresponding anthranilic acid ester **8a** and **8b** in 69% and 79% yields, respectively. Amide formation of the esters **8** with various amines was promoted by trimethylaluminum to afford the

Keywords: VEGFR-1; VEGFR-2; Benzamides; Benzamidines; VEGFR tyrosine kinases; Inhibitor.
* Corresponding author. Tel.: +81 339860221; fax: +81 359921029; e-mail: hiroyuki.nakamura@gakushuin.ac.jp

0960-894X/$ - see front matter © 2006 Elsevier Ltd. All rights reserved.
doi:10.1016/j.bmcl.2006.07.075

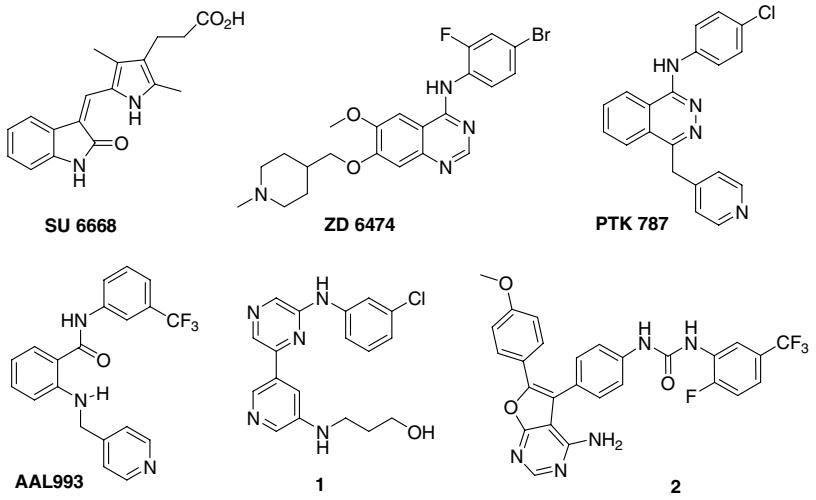

Figure 1. Structures of VEGFR tyrosine kinase inhibitors.

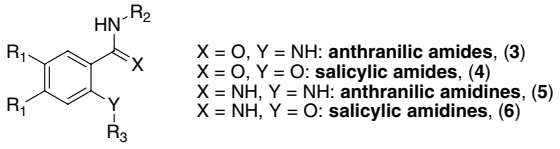

Figure 2. Design of benzamides and benzamidines as inhibitors of VEGFR tyrosine kinases.

corresponding anthranilic amides **3a**–**f** in 30–71% yields as shown in Table 1.

Salicylic amides **4a**–**f** were synthesized from 2-methoxybenzoic acids **9a** (R^1 = H) or **9b** (R^1 = MeO) as shown in Scheme 2. The 2-methoxybenzoic acids **9a**–**b** were treated with thionyl chloride, and the resulting acid chlorides reacted with various amines to afford the 2-methoxy benzoic acid amides in 50–99% yields, which underwent selective demethylation at C-2 position in the presence of boron trichloride,[11] giving the salicylic amides **10a**–**f** in 23–78% yields. The reaction of **10a**–**f** with 4-chloromethylpyridine gave the salicylic amides **4a**–**f**.[12]

Scheme 3 shows the synthesis of the salicylic amides **4g**–**h**, which were not obtained by the above synthetic scheme. Treatment of **9b** with BCl_3 gave the methyl ester **11**, which underwent ether formation with 4-chloromethylpyridine followed by amide formation with various amines using $AlMe_3$ to give the salicylic amides **4g**–**h**.

We next synthesized the anthranilic and salicylic amidines **5** and **6**. The anthranilic amidines **5a**–**f** were synthesized from 2-aminobenzonitrile **12a** or 4,5-dimethoxyl-2-aminobenzonitrile **12b** (Scheme 4). Reductive amination of **12a**–**b** with 4-pyridinecarboxaldehyde proceeded in the presence of $NaCNBH_3$, giving the corresponding benzonitriles **13a** and **13b** in 41% and 92% yields, respectively. Amidine formation of **13a**–**b** with various amines was promoted by trimethylaluminum to afford the corresponding anthranilic amidines **5a**–**f** in 30–71% yields (Table 1). Salicylic amidines **6a**–**f** were also synthesized from 2-hydroxybenzonitrile **14a** and 4,5-dimethoxyl-2-hydroxybenzonitrile **14b** along with Scheme 5. In the amidine synthesis, we examined the reaction of benzonitriles, such as **12b** and **13b**, with pyrazin-2-amine and/or pyrimidin-2-amine in order to compare with **3e** and **3f**, however, the desired amidines were not obtained.

Inhibitory activity of the anthranilic amides **3a**–**f**, salicylic amides **4a**–**h**, anthranilic amidines **5a**–**f**, and salicylic amidines **6a**–**f** was investigated by ELISA using VEGFR1 (Flt-1) and VEGFR2 (KDR).[13,14] Percents of kinase inhibition at a 10 μM concentration of compounds are shown in Table 1. Among anthranilic amides **3a**–**f**, **3b** showed 12% and 30% kinase inhibitions of Flt-1 and KDR, respectively. Salicylic amide **4a** showed significant inhibition of both Flt-1 and KDR (50% and 60%, respectively), whereas, **4b**, **4e**, and **4h** showed selective inhibition of KDR (24%, 55%, and 24%, respectively). No kinase inhibition was observed in a series of benzamidines **5** and **6**, except for **5a**, which showed 44% kinase inhibition of KDR. We also examined EGFR tyrosine kinase assay, however, no inhibition was observed in compounds **3**–**6** at a 10 μM concentration.

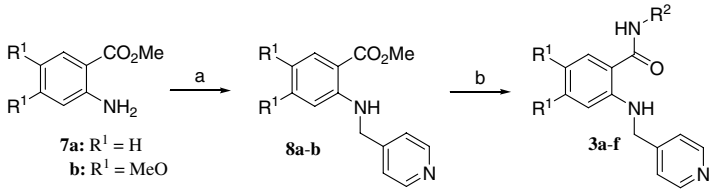

Scheme 1. Reagents: (a) 4-pyridinecarboxaldehyde, $NaCNBH_3$, MeOH, **8a**: 69%, **8b**: 79%; (b) RNH_2, $AlMe_3$, toluene, 30–71%.

Table 1. Yields and VEGFR1/2 kinase inhibitions of the anthranilic amides **3a–f**, salicylic amides **4a–h**, anthranilic amidines **5a–f**, and salicylic amidines **6a–f**

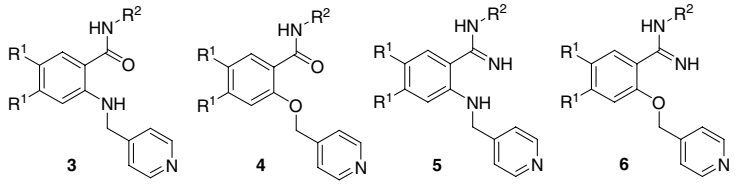

Compound	R^1	R^2	Yield (%)	% of inhibition[a]	
				Flt-1[b]	KDR[c]
3a	H		71	—	—
3b	H		30	12	30
3c	H		41	—	—
3d	MeO		59	—	—
3e	MeO		30	—	—
3f	MeO		53	—	—
4a	H	2-$CF_3C_6H_4$	35	50	60
4b	H	2-ClC_6H_4	20	—	24
4c	MeO	2-$CF_3C_6H_4$	35	—	—
4d	MeO	2-ClC_6H_4	20	—	—
4e	MeO	4-ClC_6H_4	20	3	55
4f	MeO		33	—	—
4g	MeO		33	—	—
4h	MeO		Trace	—	24
5a	H	2-$CF_3C_6H_4$	70	—	44
5b	H	4-ClC_6H_4	31	—	7
5c	H	2-ClC_6H_4	49	—	—
5d	MeO	2-$CF_3C_6H_4$	80	—	—
5e	MeO	4-ClC_6H_4	57	—	—
5f	MeO	2-ClC_6H_4	28	—	—
6a	H	2-$CF_3C_6H_4$	48	—	—
6b	H	4-ClC_6H_4	47	—	—
6c	H	2-ClC_6H_4	54	—	—
6d	MeO	2-$CF_3C_6H_4$	35	—	—
6e	MeO	4-ClC_6H_4	19	—	—
6f	MeO	2-ClC_6H_4	31	—	—
AAL993[d]				34	95 (31 nM)

[a] The inhibitory activity of compounds toward tyrosine kinases was determined by ELISA. Kinase assay was performed at a 10 μM concentration of compounds.

[b] Catalytic domain of VEGFR1 protein tyrosine kinase.

[c] Catalytic domain of VEGFR2 protein tyrosine kinase.

[d] Kinase assay was performed at a 1 μM concentration of AAL993. IC_{50} value is indicated in parentheses.

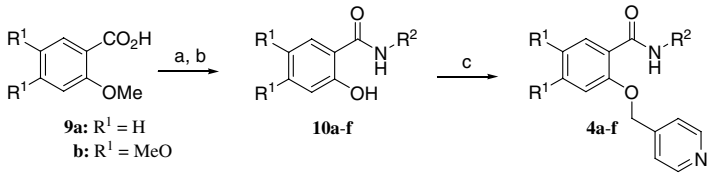

Scheme 2. Reagents: (a) i—$SOCl_2$; ii—R^2NH_2, DMAP, pyridine, 50–99%; (b) BCl_3, CH_2Cl_2, 23–78%; (c) i—KOH, H_2O; ii—4-chloromethylpyridine, 20–35%.

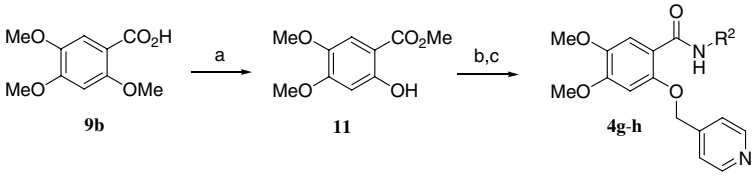

Scheme 3. Reagents and conditions: (a) i.—BCl_3, CH_2Cl_2; ii—H_2SO_4, MeOH, reflux, 79%; (b) i—KOH, H_2O; ii—4-chloromethylpyridine, 61%; (c) RNH_2, $AlMe_3$, toluene, **4g**: 33%, **4h**: <5%.

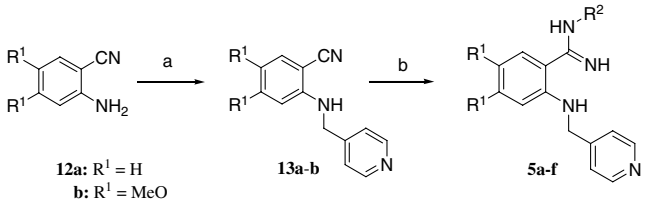

Scheme 4. Reagents and conditions: (a) 4-pyridinecarboxaldehyde, AcOH, MeOH, then $NaCNBH_3$, rt, **12a**: 41%, **12b**: 92%; (b) RNH_2, $AlMe_3$, toluene, 70 °C, 28–80%.

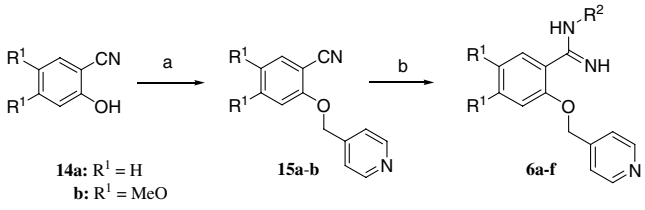

Scheme 5. Reagents and conditions: (a) i—KOH, MeOH; ii—4-chloromethylpyridine, Et_3N, DMF, 140 °C, **14a**: 41%, **14b**: 46%; (b) RNH_2, $AlMe_3$, toluene, 70 °C, 47–54%.

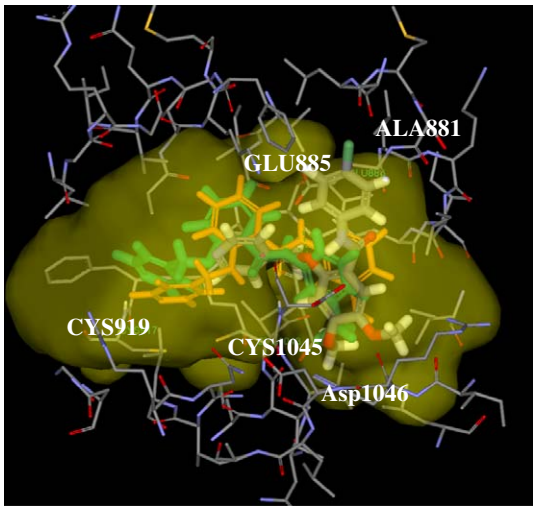

Figure 3. Docking modes of **4a** (green) and **4e** (gray) overlaid with the binding conformation of AAL993 (orange) into the active site of VEGFR2 kinase domain. Docking model was calculated by the DS modeling 1.2 based on the X-ray analysis data of VEGFR2 tyrosine kinase with aminopyrimidine **2**[8] (PDB code: 1YWN). The yellow cloud shows a ligand-binding site calculated by the site finding module.

In order to better understand the structure-activity relationship between the VEGFR2 tyrosine kinase inhibition and the possible binding modes of the salicylic amides **4a** and **4e**, we performed molecular docking experiments of AAL993, **4a** and **4e** with the ligand-binding site of VEGFR2 kinase (PDB code 1YWN). According to our docking simulation as shown in Figure 3, **4a** would interact with VEGFR2 kinase domain through hydrogen bonds between the pyridine–N and the backbone-NH of Cys919 in the hinge region of the kinase, the salicylamide–C=O and the backbone–NH of Asp1046 of the DFG-loop, and the salicylamide–NH with the side-chain carboxylate of Glu885 of helix–C, as indicated by the green stick; the ligscore2[15] was calculated as 5.33, which is smaller than that of AAL993 (the ligscore2 = 5.86). The salicylic amide **4e** showed a different binding mode as indicated by gray bold stick in Figure. 3. The 4,5-dimethoxysalicylic group of **4e** occupied the binding site of $CF_3C_6H_4$ groups of **4a** and AAL993, and the 4-ClC_6H_4 group was located near Ala879. The ligscore2 of **4e** was calculated as 4.78.

In conclusion, we succeeded in the synthesis of a series of anthranilic amides, salicylic amides, anthranilic amidines, and salicylic amidines. Among the compounds synthesized, the salicylic amide **4a** possessed inhibitory activities of both Flt-1 and KDR, whereas, the salicylic amide **4e** and the anthranilic amidine **5a** were found as selective inhibitors of VEGFR-2 tyrosine kinases. Two methoxy groups substituted on the salicylic ring of **4e** enhanced the selectivity of VEGFR2 kinase inhibition in comparison with **4a**. We believe that the current finding would be important for designs of tyrosine kinase-targeted new therapeutic agents.

Acknowledgments

This work was supported by the Ministry of Education, Science, Sports, Culture and Technology, Grant-in-Aid for the Screening Committee of New Anticancer Agents on Priority Area 'Cancer' for the protein kinase assay and for Scientific Research (A) for young scientists (No. 16685017) from Japan.

References and notes

1. Risau, W. *Nature* **1997**, *386*, 671.
2. (a) Manley, P. W.; Bold, G.; Brüggen, J.; Frendrich, G.; Furet, P.; Mestan, J.; Schnell, C.; Stolz, B.; Meyer, T.; Meyhack, B.; Stark, J.; Strauss, A.; Wood, J. *Biochim. Biophys. Acta* **2004**, *16975*, 17; (b) Lawrence, D. S.; Niu, J. *Pharmacol. Ther.* **1998**, *77*, 81.
3. (a) Abdollahi, A.; Lipson, K. E.; Han, X.; Krempien, R.; Trinh, T.; Weber, K. J.; Hahnfeldt, P.; Hlatky, L.; Debus, J.; Howlett, A. R.; Huber, P. E. *Cancer Res.* **2003**, *63*, 3755; (b) Sun, L.; Tran, N.; Liang, C.; Hubbard, S.; Tang, F.; Lipson, K.; Schreck, R.; Zhou, Y.; McMahon, G.; Tang, C. *J. Med. Chem.* **2000**, *43*, 2655.
4. (a) Hennequin, L. F.; Stokes, E. S. E.; Thomas, A. P.; Johnstone, C.; Plé, P. A.; Ogilvie, D. J.; Dukes, M.; Wedge, S. R.; Kendrew, J.; Curwen, J. O. *J. Med. Chem.* **2002**, *45*, 1300; (b) Hennequin, L. F.; Thomas, A. P.; Johnstone, C.; Stokes, E. S. E.; Plé, P. A.; Lohmann, J.-J. M.; Ogilvie, D. J.; Dukes, M.; Wedge, S. R.; Kendrew, J.; Lambert van der Brempt, C. *J. Med. Chem.* **1999**, *42*, 5369.
5. (a) Drevs, J.; Muller-Driver, R.; Wittig, C.; Fuxius, S.; Esser, N.; Hugenschmidt, H.; Konerding, M. A.; Allegrini, P. R.; Wood, J.; Hennig, J.; Unger, C.; Marme, D. *Cancer Res.* **2002**, *62*, 4015; (b) Bold, G.; Altman, K.-H.; Frei, J.; Lang, M.; Manley, P. W.; Traxler, P.; Wietfeld, B.; Bruggen, J.; Buchdunger, E.; Cozens, R.; Ferrari, S.; Furet, P.; Hofmann, F.; Martiny-Baron, G.; Mestan, J.; Rosel, J.; Sills, M.; Stover, D.; Acemoglu, F.; Boss, E.; Emmenegger, R.; Lasser, L.; Masso, E.; Roth, R.; Schlachter, C.; Vetterli, W.; Wyss, D.; Wood, J. M. *J. Med. Chem.* **2000**, *43*, 2310.
6. Manley, P. W.; Furet, P.; Bold, G.; Bruggen, J.; Mestan, J.; Meyer, T.; Schnell, C. R.; Wood, J.; Haberey, M.; Huth, A.; Kruger, M.; Menrad, A.; Ottow, E.; Seidelmann, D.; Siemeister, G.; Thierauch, K-H. *J. Med. Chem.* **2002**, *45*, 5687.
7. Kou, G.-H.; Wang, A.; Emauel, S.; DeAngelis, A.; Zhang, R.; Connolly, P. J.; Murray, W. V.; Gruninger, R. H.; Sechler, J.; Fuentes-Pesquera, A.; Johnson, D.; Middleton, S. A.; Jolliffe, L.; Chen, X. *J. Med. Chem.* **2005**, *48*, 1886.
8. Miyazaki, Y.; Matsunaga, S.; Tang, J.; Maeda, Y.; Nakano, M.; Philippe, R. J.; Shibahara, M.; Liu, W.; Sato, H.; Wang, L.; Nolte, R. T. *Bioorg. Med.Chem. Lett.* **2005**, *15*, 2203.
9. (a) Manley, P. W.; Bold, G.; Fendrich, G.; Furet, P.; Mestan, J.; Meyer, T.; Meyhack, B.; Stark, W.; Strauss, A.; Wood, J. *Cell. Mol. Biol. Lett.* **2003**, *8*, 532; (b) Manley, P. W.; Bold, G.; Brüggen, J.; Fendrich, G.; Furet, P.; Mestan, J.; Schnell, C.; Stolz, B.; Meyer, T.; Meyhack, B.; Stark, W.; Strauss, A.; Wood, J. *Biochim. Biophys. Acta* **2004**, *1697*, 17.
10. (a) Asano, T.; Yoshikawa, T.; Nakamura, H.; Uehara, Y.; Yamamoto, Y. *Bioorg. Med. Chem. Lett.* **2004**, *14*, 2299; (b) Asano, T.; Yoshikawa, T.; Usui, T.; Yamamoto, H.; Yamamoto, Y.; Uehara, Y.; Nakamura, H. *Bioorg. Med. Chem.* **2004**, *12*, 3529; (c) Asano, T.; Nakamura, H.; Uehara, Y.; Yamamoto, Y. *ChemBioChem* **2004**, *5*, 483.
11. Dean, F. M.; Goodchild, J.; Houghton, J. A.; Martin, R. B.; Parton, B.; Price, A. W.; Somvichien, N. *Tetrahedron Lett.* **1966**, *7*, 4153.
12. Ibrahim, A. Y.; Behbehani, H.; Ibrahim, R. M.; Malhas, R. *Tetrahedron* **2003**, *59*, 7273.
13. Iwata, K. K.; Jani, J. P.; Provoncha, K.; Kath, J. C.; Liu, Z.; Moyer, J. D. *Cancer Res.* **2003**, *63*, 4450.
14. EIA/RIA stripwell™ plates (Corning) were coated by incubation overnight at 4 °C with 100 μl/well of 50 μg/ml poly(Glu:Tyr,4:1) peptide (Sigma) in PBS. The kinase reaction was performed in the plates by addition of 50 μl of kinase buffer (50 mM HEPES, 125 mM NaCl, 10 mM $MgCl_2$, pH 7.4) containing 100 μM of ATP, 10 ng of recombinant Flt-1 or KDR (Invitrogen, catalytic domain of VEGFR1 and VEGFR2, respectively), and a compound (10 μM). After 20 min, the plates were washed three times with wash buffer (0.1% Tween 20 in PBS) and incubated for 20 min with 50 μl/well of 0.2 μg/ml HRP conjugated anti-phosphotyrosine antibody (Santa Cruz). After two washes, the plates were developed by addition of 50 μl/well Tetramethylbenzidine (Sigma) and stopped by addition of 50 μl/well of 2 N H_2SO_4. The absorbance at 450 nm was measured by a 96-well plate reader (Tecan).
15. LigScore2 is a fast, simple scoring function for predicting protein–ligand binding affinities. The functional form of LigScore is simple and contains the CFF force field using grid-based energy calculations with the improved interpolation method; see: Wang, R.; Lu, Y.; Wang, S. *J. Med. Chem.* **2003**, *46*, 2287.